

# Enhancing Signal Discontinuities with Shearlets: An Application to Corner Detection

Miguel Alejandro Duval-Poo<sup>1</sup>, Francesca Odone<sup>1(✉)</sup>, and Ernesto De Vito<sup>2</sup>

<sup>1</sup> DIBRIS - Università Degli Studi di Genova, Genoa, Italy  
francesca.odone@unige.it

<sup>2</sup> DIMA - Università Degli Studi di Genova, Genoa, Italy

**Abstract.** Shearlets are a relatively new and very effective multi-resolution framework for signal analysis able to capture efficiently the anisotropic information in multivariate problem classes. For this reason, Shearlets appear to be a valid choice for multi-resolution image processing and feature detection. In this paper we provide a brief review of the theory, referring in particular to the problem of enhancing signal discontinuities. We then discuss the specific application to corner detection, and provide a novel algorithm based on the concept of a cornerness measure. The appropriateness of the algorithm in detecting good matchable corners is evaluated on benchmark data including different image transformations.

## 1 Introduction

Multi-resolution methods, which are concerned with the representation and the analysis of images at multiple resolutions, are very appealing and effective in image processing since image features that are difficult to detect at one resolution may be easily detectable at another. In this general framework, Wavelets have often been chosen to represent the image content and, more specifically, to enhance signal discontinuities [14]. However, Wavelets are known to have a limited capability in dealing with directional information. In recent years, several methods were introduced to overcome these limitations (see, for instance, [2, 13, 18, 20]). Among those, the *Shearlet representation* offers a unique combination of some highly desirable properties: it has a single or finite set of generating functions, it provides optimally sparse representations for a large class of multi-dimensional data, it allows the use of compactly supported analyzing functions both in the space and frequency domain. Last, but not less important, it has fast algorithmic implementations and it allows a unified treatment of the continuum and digital realms. For these reasons, in this work we choose Shearlets as a reference framework for feature detection.

In this paper we summarize some of Shearlets theoretical and computational properties, while referring in particular to the problem of enhancing image singularities. We then apply these findings to the corner detection problem which has not been fully addressed yet within the Shearlet framework. We take inspiration from [22], but we adopt a different algorithm to compute the digitalized

Shearlet transform, which was first introduced in [8] for segmentation problems. With respect to the latter we choose a *mother function* which is more suitable for enhancing signal discontinuities.

There are several approaches for detecting corners in images. Since the pioneering work of Harris and Stephens [7], and later of Shi and Tomasi [21], the structure tensor of image gradients, also known as the *autocorrelation matrix*, has become popular for corner detection. A recent review on interest points, and corners in particular, is [1]. Wavelets have been applied to corner detection [3, 17], although their limited capability in dealing with directional information is critical for this application. In order to overcome this limitation, orientation sensitive wavelets, such as the Log-Gabor wavelets, have been adopted [5]. Here we present an alternative way for addressing the problem effectively by selecting a more appropriate orientation selective transform.

The paper is organized as follows: in Section 2 we briefly review the Shearlet transform in the continuous and discrete case. In Section 3 we address the general issue of detecting signal discontinuities with Shearlets, while in Section 4 we propose procedures for corner detection, whose effectiveness is discussed in Section 5 following the Oxford evaluation procedure [16]. Section 6 is left to a final discussion and to an account of future works.

## 2 A Review of the Shearlet Transform

In this section we review the main properties of Shearlets, referring the interested reader to [11]. A shearlet is generated by the dilation, shearing and translation of a function  $\psi \in L^2(\mathbb{R}^2)$ , called the *mother shearlet*, in the following way

$$\psi_{a,s,t}(x) = a^{-3/4} \psi(A_a^{-1} S_s^{-1}(x - t)) \quad (1)$$

where  $t \in \mathbb{R}^2$  is a translation,  $A_a$  is a *scaling* (or *dilation*) matrix and  $S_s$  a *shearing* matrix defined respectively by

$$A_a = \begin{pmatrix} a & 0 \\ 0 & \sqrt{a} \end{pmatrix} \quad S_s = \begin{pmatrix} 1 & -s \\ 0 & 1 \end{pmatrix},$$

with  $a \in \mathbb{R}^+$  and  $s \in \mathbb{R}$ . The anisotropic dilation  $A_a$  controls the scale of the Shearlets, by applying a different dilation factor along the two axes. The shearing matrix  $S_s$ , not expansive, determines the orientation of the Shearlets. The normalization factor  $a^{-3/4}$  ensures that  $\|\psi_{a,s,t}\| = \|\psi\|$ , where  $\|\psi\|$  is the Hilbert norm in  $L^2(\mathbb{R}^2)$ .

The *Shearlet transform*  $\mathcal{SH}(f)$  of a signal  $f \in L^2(\mathbb{R}^2)$  is defined by

$$\mathcal{SH}(f)(a, s, t) = \langle f, \psi_{a,s,t} \rangle, \quad (2)$$

where  $\langle f, \psi_{a,s,t} \rangle$  is the scalar product in  $L^2(\mathbb{R}^2)$ . A possible classical choice for the *mother Shearlet*  $\psi$  is

$$\hat{\psi}(\omega_1, \omega_2) = \hat{\psi}_1(\omega_1) \hat{\psi}_2\left(\frac{\omega_2}{\omega_1}\right) \quad (3)$$

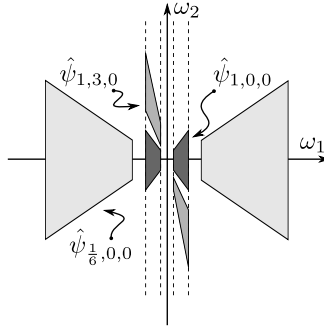


**Fig. 1.** Support of the Shearlets  $\hat{\psi}_{a,s,t}$  in the frequency domain.

where  $\hat{\psi}$  is the Fourier transform of  $\psi$ , and  $\hat{\psi}_1, \hat{\psi}_2$  are usually two compactly supported functions in the one-dimensional frequency domain. The mother Shearlet in the frequency domain becomes

$$\hat{\psi}_{a,s,t}(\omega_1, \omega_2) = a^{3/4} \hat{\psi}_1(a\omega_1)\hat{\psi}_2\left(\frac{\omega_2 - s\omega_1}{\sqrt{a}\omega_1}\right) e^{-2\pi it \cdot (\omega_1, \omega_2)} \tag{4}$$

and it has a support on two trapezoids at scale  $a$  oriented along a line of slope  $s$  (Fig. 1). The Shearlet transform can be rewritten as

$$\mathcal{SH}(f)(a, s, t) = a^{3/4} \int_{\hat{\mathbb{R}}^2} \hat{f}(\omega_1, \omega_2)\hat{\psi}_1(a\omega_1)\hat{\psi}_2\left(\frac{\omega_2 - s\omega_1}{\sqrt{a}\omega_1}\right) e^{2\pi it \cdot (\omega_1, \omega_2)} d\omega_1 d\omega_2.$$

The mother function  $\psi$  satisfies some technical condition, which we do not discuss in detail, see [11]. In the following we assume that  $\psi_1$  is a one-dimensional wavelet and  $\hat{\psi}_2$  is a bump function whose support is in  $[-1, 1]$ .

The Shearlet transform is able to capture the geometry of signal singularities through its asymptotic decay at fine scales ( $a \rightarrow 0$ ). A group of theoretical results [6, 12] show that the Shearlet transform precisely describes the geometric information of edges and other singular points of an image through their asymptotic behavior at fine scales. Explicitly, the Shearlet coefficient  $\mathcal{SH}(\mathcal{I})(a, s, t)$  goes to zero faster than any power of  $a$  either if  $t$  is a regular point (for any  $s$ ) or if  $t$  is an edge point and  $s \neq s_0$  where  $s_0$  is the normal orientation of the edge. If  $t$  is an edge and  $s = s_0$ , the decay is of the order  $a^{3/4}$ . A similar behaviour holds if  $t$  is a corner point and  $s$  coincides with one of the normal directions of the corner, otherwise the decay is  $O(a^{9/4})$ .

For numerical implementation, it is useful to restrict the range of  $a$  and  $s$  to bounded intervals. This is achieved by a suitable tiling of the frequency plane

$$\begin{aligned} \mathcal{C}_h &= \{(\omega_1, \omega_2) \in \mathbb{R}^2 : |\omega_2/\omega_1| \leq 1, |\omega_1| > 1\}, \\ \mathcal{C}_v &= \{(\omega_1, \omega_2) \in \mathbb{R}^2 : |\omega_1/\omega_2| \leq 1, |\omega_2| > 1\}, \\ \mathcal{R} &= \{(\omega_1, \omega_2) \in \mathbb{R}^2 : |\omega_1|, |\omega_2| \leq 1\}. \end{aligned}$$

For each cone  $\mathcal{C}_{h,v}$  there is a corresponding mother Shearlet

$$\begin{aligned}\hat{\psi}^h(\omega_1, \omega_2) &= \hat{\psi}_1(\omega_1)\hat{\psi}_2\left(\frac{\omega_2}{\omega_1}\right)\chi_{\mathcal{C}_h} \\ \hat{\psi}^v(\omega_1, \omega_2) &= \hat{\psi}_1(\omega_2)\hat{\psi}_2\left(\frac{\omega_1}{\omega_2}\right)\chi_{\mathcal{C}_v}\end{aligned}$$

where  $\chi_{\mathcal{C}_{h,v}}$  is 1 on  $\mathcal{C}_{h,v}$  and 0 outside. The low frequency region  $\mathcal{R}$  can be handled by a scaling function  $\hat{\phi}(\omega_1, \omega_2)$ . This construction is usually called cone-adapted Shearlets.

The next step is to provide a discretization sampling of  $a, s$  and  $t$ . In the literature there are many different discretization schemes. In this paper we adopt the Fast Finite Shearlet Transform (FFST) [8] which performs the entire Shearlet construction in the Fourier domain. In this scheme, the signal is discretized on a square on size  $N$ , which is independent of the dilation and shearing parameter, whereas the scaling, shear and translation parameters are discretized as

$$\begin{aligned}a_j &= 2^{-j}, \quad j = 0, \dots, j_0 - 1, \\ s_{j,k} &= k2^{-j/2}, \quad -\lfloor 2^{j/2} \rfloor \leq k \leq \lfloor 2^{j/2} \rfloor, \\ t_m &= \left(\frac{m_1}{N}, \frac{m_2}{N}\right), \quad m \in \mathcal{I}\end{aligned}$$

where  $j_0$  is the number of considered scales and  $\mathcal{I} = \{(m_1, m_2) : m_1, m_2 = 0, \dots, N - 1\}$ . With these notations the Shearlet system becomes

$$\psi_{j,k,m}^x(x) = \psi_{a_j, s_{j,k}, t_m}^x(x)$$

where  $x = h$  or  $x = v$ .

The *discrete Shearlet transform* of a digital image  $\mathcal{I}$  is now defined as

$$\mathcal{SH}(\mathcal{I})(j, k, m) = \begin{cases} \langle \mathcal{I}, \phi_m \rangle \\ \langle \mathcal{I}, \psi_{j,k,m}^h \rangle \\ \langle \mathcal{I}, \psi_{j,k,m}^v \rangle \end{cases}$$

where  $j = 0, \dots, j_0 - 1$ ,  $|k| \leq \lfloor 2^{j/2} \rfloor$ ,  $m \in \mathcal{I}$ . Based on the Plancherel formula  $\langle f, g \rangle = \frac{1}{N^2} \langle \hat{f}, \hat{g} \rangle$ , the discrete shearlet transform can be efficiently computed by applying the 2D fast Fourier transform (**fft**) and its inverse (**ifft**). Thus, a *discrete Shearlet transform algorithm* can be summarized as

$$\mathcal{SH}(\mathcal{I})(j, k, m) = \begin{cases} \text{ifft}(\hat{\phi}(\omega_1, \omega_2)\text{fft}(\mathcal{I}))(m) \\ \text{ifft}(\hat{\psi}_1(2^{-j}\omega_1)\hat{\psi}_2(2^{j/2}\frac{\omega_2}{\omega_1} - k)\text{fft}(\mathcal{I}))(m) \\ \text{ifft}(\hat{\psi}_1(2^{-j}\omega_2)\hat{\psi}_2(2^{j/2}\frac{\omega_1}{\omega_2} - k)\text{fft}(\mathcal{I}))(m) \end{cases}. \quad (5)$$

### 3 Detecting Discontinuities with Shearlets

In this section we discuss the ability of Shearlets to enhance local signal discontinuities.



**Fig. 2.** Enhancement of signal discontinuities provided by Shearlets: two example images and the results obtained by choosing the  $\hat{\psi}_1$  as the Lemarie-Meyer wavelet (center) or the Mallat wavelet (right).

**Shearlets for Enhancing Discontinuities.** In choosing the function  $\psi_1$  we adopt the Mallat wavelet [15], a family of one dimensional wavelets which share the same properties of the first derivative of the Gaussian:

$$\hat{\psi}_1(\omega) = i\omega \left( \frac{\sin(\omega/4)}{\omega/4} \right)^{2n+2}. \tag{6}$$

This choice is alternative to the classical Lemarie-Meyer wavelet [4, 8] which is not optimal for edge detection since the Lemarie-Meyer wavelet is an even function and thus its Shearlet transforms suffer from large side-lobes around prominent edges, which interfere with the detection of the edge location (see Fig. 2). As for  $\psi_2$ , instead, any smooth function with compact support in the frequency domain can be considered. In our case we used the same bump function as in [4, 8].

**Enhancing Discontinuities at Fixed Scales.** Signal discontinuities can be identified as those points  $m \in \mathcal{I}$  which, at scale  $j$ , the function  $\mathcal{E}_j(m)$  has large values, with

$$\mathcal{E}_j(m)^2 = \sum_k (\mathcal{SH}(\mathcal{I})(j, k, m))^2. \tag{7}$$

$\mathcal{SH}(\mathcal{I})(j, k, m)$  denotes the discrete Shearlet transform of  $\mathcal{I}$  in Eq. (5).

**Estimating the Discontinuities Orientation at Fixed Scales.** The Shearlet transform provides naturally this type of information, which can be easily obtained at a fixed scale  $j$  by finding the index  $k$  that maximizes  $\mathcal{SH}(\mathcal{I})(j, k, m)$ ,

$$\theta_j(m) = \arg \max_k |\mathcal{SH}(\mathcal{I})(j, k, m)|. \tag{8}$$

Fig. 3 shows different orientations at different scales  $j$ . The estimated directions are color coded, i.e. each color represents a specific direction summarized in the colorbar at the right of the figure. As we can observe, the Shearlet transform

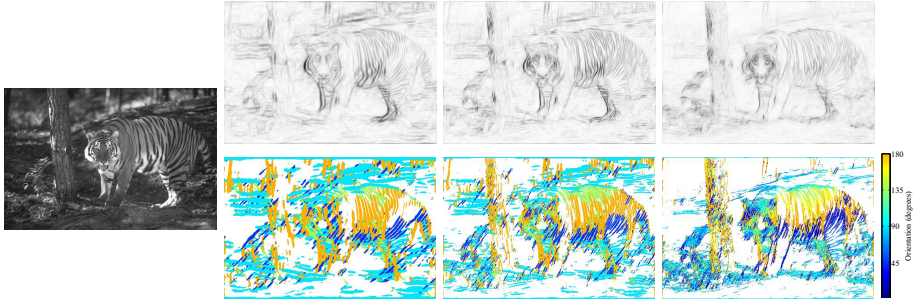


**Fig. 3.** Image discontinuities across scales. Top: Shearlet coefficients - Eq. (7). Bottom: Orientations - Eq. (8). Coarse to fine from left to right.

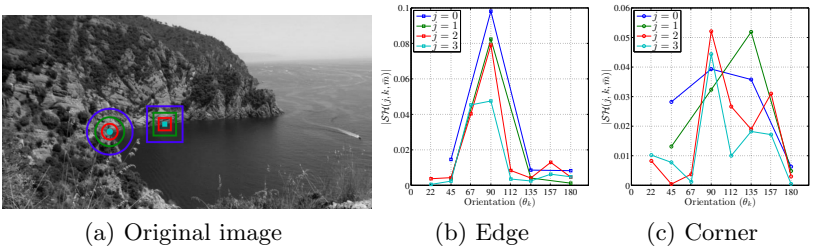


**Fig. 4.** Shearlet orientation patterns for an edge (square) and a corner (circle).

accurately estimates the orientation. In addition, it can be noticed how accuracy increases at fine scales ( $j \rightarrow 3$ ) due to the fact that at fine scales more shears  $k$  have to be considered,  $-\lfloor 2^{j/2} \rfloor \leq k \leq \lfloor 2^{j/2} \rfloor$ .

**Analysing Discontinuities Across Scales.** Orientation is an important cue to classify different types of signal discontinuities. To this purpose, we may analyze how the Shearlets coefficients vary across different orientations. Fig. 4 shows a comparison of the orientation patterns in the case of an edge (square) and a corner (circle) in a natural image. Let us first consider a fixed scale  $j = 2$  (red plots). As we can observe, for the edge point a strong Shearlet response is obtained on one direction only, while for the corner point it can be observed strong Shearlet responses at two different, almost perpendicular, orientations. If we perform the analysis across scales, it can be seen how on the edge point the strongest Shearlet response is maintained on one direction only with the exception of the finest scale where two high responses are obtained on two close orientations. Instead, on the corner point, the two orientations with the strongest Shearlet response slightly vary across scales. This is an expected behavior since, depending of the scale at which the analysis is performed, a corner point can have different main orientations.

## 4 Corner Detection with Shearlets

Corner patterns are associated with signal discontinuities in at least two directions and it is reflected on the behavior of Shearlet coefficients across different orientations, as discussed in the previous section. In this work we favor corners associated with at least two large coefficients, with a preference for patterns where such coefficients are at about 90 degrees to one another (the “ideal” corner).

Considering a generic image point  $m$ , at a fixed scale we compute a weighted sum of its Shearlet coefficients across shears, where each weight is a value that represents how *perpendicular* is the orientation of the shear with the orientation of the shear with the maximum Shearlet response for that point. To this purpose, we define a *cornerness measure*  $\mathcal{CM}$  for a point  $m \in \mathcal{I}$  and for a fixed scale  $j$  in the following way

$$\mathcal{CM}_j(m) = \sum_{u \in W(m)} \sum_k |\mathcal{SH}(j, k, u)| \sin(|\theta_k - \theta_{k_{\max}}|)$$

where  $\mathcal{SH}(j, k, u)$  represents the discrete Shearlet transform coefficient for a point  $u$  in a neighborhood of  $m$ , at scale  $j$  and shearing  $k$ ,  $\theta_k$  is the angle associated to the shearing  $k$ ,  $k_{\max} = \arg \max_k |\mathcal{SH}(j, k, m)|$  and  $W(m)$  is a window centered at point  $m$  of an appropriate size. Then we may aggregate the cornerness measure at different scales:  $\mathcal{CM}(m) = \sum_j \mathcal{CM}_j(m)$ . In this way detected corner points that persist across scales are reinforced. Alg. 1 describes a sketch of the algorithm.

Taking the advantage of the multi-scale representation produced by the Shearlets, we may associate an appropriate scale to each detected corner  $m \in \mathcal{C}$ :

$$\bar{j} = \arg \max_j K_j \sum_k |\mathcal{SH}(j, k, m)| \quad (9)$$

where  $K_j$  is a normalization factor that depends on the scale  $j$ . Fig. 5 shows the result of the Shearlet multi-scale corner detection with automatic scale selection.

## 5 Experimental Results

In this section we assess the effectiveness of the corner detection procedure. The evaluation is based on the standard Mikolajczyk’s software framework<sup>1</sup>. Image sequences are provided, each one containing 6 images of natural textured scenes with increasing geometric and photometric transformations. In our analysis we discarded those that are not applicable in our scenario that does not consider large zooming and rotations (normally addressed by appropriate descriptors). For the evaluation metrics [16] we consider:

- The *number of correspondences*  $|CR_{1i}|$ , is the cardinality of the set containing all the corner points correspondences between image  $\mathcal{I}_1$  and the evaluated

<sup>1</sup> <http://www.robots.ox.ac.uk/~vgg/research/affine/>

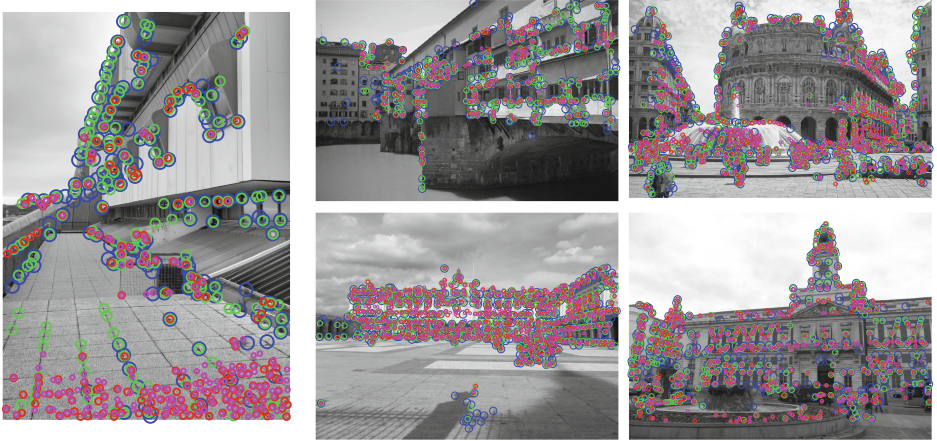


**Fig. 5.** Shearlet corner detection with automatic scale estimation - sample outputs:  $j = 0$  (Blue);  $j = 1$  (Green);  $j = 2$  (Red);  $j = 3$  (Magenta).

---

**Algorithm 1.** Shearlet Corner Detection.

**Input**  $\mathcal{I}$ : input image,  $j_0$ : number of scales considered,  $t$ : threshold.

**Output**  $\mathcal{C}$ : set of detected corner points.

---

```

1: procedure SMCD( $\mathcal{I}, j_0, t$ )
2:    $\mathcal{C} = \{\}$ ;
3:    $\mathcal{SH} = \text{dst}(\mathcal{I})$ ; // Discrete Shearlet Transform as in Eq. (5)
4:   for all  $m \in \mathcal{I}$  do
5:      $\mathcal{CM}(m) = \sum_j \sum_{u \in W(m)} \sum_k |\mathcal{SH}(j, k, u)| \sin(|\theta_k - \theta_{k_{\max}}|)$ ; //Multi-Scale
    Cornerness
6:   end for
7:    $\text{nonmaxsup}(\mathcal{CM})$ ; // Non Maxima Suppression as in [9]
8:   for all  $m \in \mathcal{I}$  do
9:     if  $\mathcal{CM}(m) > t$  then // Corner detection
10:       $\mathcal{C} = \mathcal{C} \cup (m)$ ;
11:    end if
12:  end for
13:  return  $\mathcal{C}$ ;
14: end procedure

```

---

image  $\mathcal{I}_i$ . To estimate it, we employ the homography  $H_{1_i}$  which is provided with the images and count the number of corners of image  $\mathcal{I}_i$  which are close to corners from  $\mathcal{I}_1$ , after  $H_{1_i}$  has been applied.

- The *repeatability score*  $RS_i$  for an image  $\mathcal{I}_i$  is the ratio of the number of correspondences and the minimum number of corners detected in the images:

$$RS_i = \frac{|CR_{1_i}|}{\min(|\mathcal{C}_1|, |\mathcal{C}_i|)}.$$

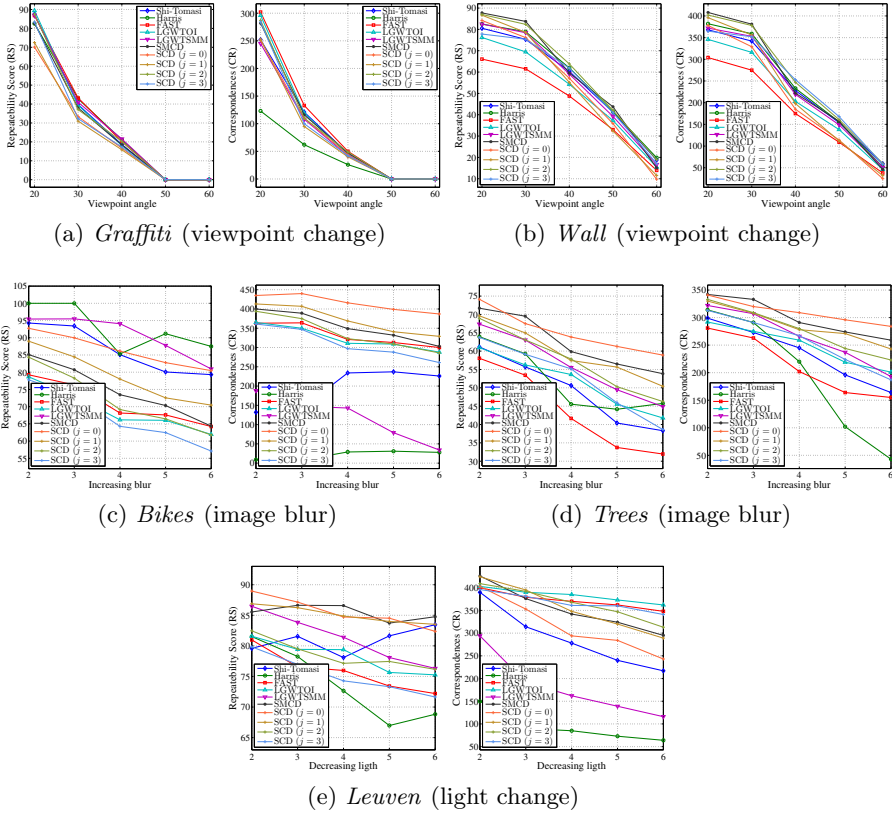


**Fig. 6.** Comparison of different corner detectors on five image sequences.

In this experimental analysis we consider the corner detection algorithm across scales that we propose (Alg. 1 - reported in the following as SMCD) as well as a variant of it where  $j$  is fixed and the only change in the algorithm is the summation across scales which is not needed (henceforth SCD). As a threshold we set 10% of the cornerness measure maximum value of each image. If more than 500 detected corner points remains, only the 500 points with the maximum cornerness measure are selected. We compare our algorithms with the classical *Harris* [7] and *Shi-Tomasi* [21], the two methods *LGWTOI* and *LGWTSMM* proposed in [5] based on Log-Gabor wavelets, and the more recent *FAST* [19]. The results are reported in Fig. 6:

- *View-point changes*: in (a) different corner detection methods perform in a similar way, with a slightly higher number of correspondences in *FAST* slightly outperforms the rest. In (b) *SMCD* and *SCD* at scale  $j = 1, 2$  obtain a higher repeatability score and number of correspondences.
- *Image blur*: in (c) *Harris* and *LGWTSMM* obtain a very high repeatability score but with the lowest number of correspondences. The best trade-off

between the two different metrics is achieved by SCD at the coarsest scale  $j = 0$ . Coherent results are noticeable in (d), where we also observe a remarkable performance of our multi-scale variant SMCD.

- *Illumination changes*: in (e) we see how many methods (LGWTOI, FAST, SMCD and SCD with  $j = 2, 3$ ) obtained the high correspondences, but the best trade-off with the repetibility score is achieved by SMCD.

## 6 Discussion

In this paper we addressed the problem of enhancing image singularities with the Shearlet transform.

Shearlets are capable of capturing anisotropic information in multivariate functions and are thus particularly appropriate for the detection of directional sensitive features. We applied our analysis to the corner detection problem and sketched an algorithm which allowed us to detect meaningful corner features at a fixed scale and at multiple scales. The expressive power of the adopted framework allowed us also to associate a scale with each detected key point. We assessed our corner detection algorithm comparing our results with state of the art methods. The analysis illustrated the appropriateness of our algorithm in detecting matchable corners across different image transformations, with very good performances in particular for blur and illumination changes.

We are currently working on a fully multi-scale corner detection pipeline, which includes an optimal scale selection and a suppression of multiple corners across scales, comparable with the scale-space approach. The general framework adopted will allow us in the future to detect other types of image features (such as blob-like features) and space-time features (such as STIP).

Our approach relies on classical choices for the mother Shearlet, but interesting alternatives are available and would be worth investigating in future works. For instance, compactly supported Shearlets [10] have been recently shown to have nice properties for edge detection [12].

## References

1. Aanes, H., Dahl, A.L., Pedersen, K.S.: Interesting interest points. *IJCV* (2011)
2. Candes, E.J., Donoho, D.L.: New tight frames of curvelets and optimal representations of objects with piecewise  $c_2$  singularities. *Communications on Pure and Applied Mathematics* **57**(2), 219–266 (2004)
3. Chen, C.H., Lee, J.S., Sun, Y.N.: Wavelet transformation for gray-level corner detection. *Pattern Recognition* **28**(6), 853–861 (1995)
4. Easley, G., Labate, D., Lim, W.Q.: Sparse directional image representations using the discrete shearlet transform. *Applied and Computational Harmonic Analysis* **25**(1), 25–46 (2008)
5. Gao, X., Sattar, F., Venkateswarlu, R.: Multiscale corner detection of gray level images based on log-gabor wavelet transform. *IEEE Transactions on Circuits and Systems for Video Technology* **17**(7), 868–875 (2007)

6. Guo, K., Labate, D.: Characterization and analysis of edges using the continuous shearlet transform. *SIAM Journal on Imaging Sciences* **2**(3), 959–986 (2009)
7. Harris, C., Stephens, M.: A combined corner and edge detector. In: *Alvey Vision Conference*, Manchester, UK, vol. 15, p. 50 (1988)
8. Häuser, S., Steidl, G.: Fast finite shearlet transform: a tutorial. *ArXiv* (1202.1773) (2014)
9. Kitchen, L., Rosenfeld, A.: Gray-level corner detection. *Pattern Recognition Letters* **1**(2), 95–102 (1982)
10. Kittipoom, P., Kutyniok, G., Lim, W.Q.: Construction of compactly supported shearlet frames. *Constr. Approx.* **35**(1), 21–72 (2012)
11. Kutyniok, G., Labate, D.: *Shearlets: Multiscale analysis for multivariate data*. Springer (2012)
12. Kutyniok, G., Petersen, P.: Classification of edges using compactly supported shearlets. *ArXiv* (1411.5657) (2014)
13. Labate, D., Lim, W.Q., Kutyniok, G., Weiss, G.: Sparse multidimensional representation using shearlets. In: *Optics & Photonics 2005*, pp. 59140U–59140U. International Society for Optics and Photonics (2005)
14. Mallat, S., Hwang, W.L.: Singularity detection and processing with wavelets. *IEEE Transactions on Information Theory* **38**(2), 617–643 (1992)
15. Mallat, S., Zhong, S.: Characterization of signals from multiscale edges. *IEEE Transactions on Pattern Analysis and Machine Intelligence* **14**(7), 710–732 (1992)
16. Mikolajczyk, K., Tuytelaars, T., Schmid, C., Zisserman, A., Matas, J., Schaffalitzky, F., Kadir, T., Van Gool, L.: A comparison of affine region detectors. *International Journal of Computer Vision* **65**(1–2), 43–72 (2005)
17. Pedersini, F., Pozzoli, E., Sarti, A., Tubaro, S.: Multi-resolution corner detection. In: *ICIP*, pp. 881–884 (2000)
18. Po, D.D., Do, M.N.: Directional multiscale modeling of images using the contourlet transform. *Image Processing* **15**(6), 1610–1620 (2006)
19. Rosten, E., Porter, R., Drummond, T.: Faster and better: A machine learning approach to corner detection. *IEEE Transactions on Pattern Analysis and Machine Intelligence* **32**(1), 105–119 (2010)
20. Selesnick, I.W., Baraniuk, R.G., Kingsbury, N.C.: The dual-tree complex wavelet transform. *IEEE Signal Processing Magazine* **22**(6), 123–151 (2005)
21. Shi, J., Tomasi, C.: Good features to track. In: *Proceedings of the 1994 IEEE Computer Society Conference on Computer Vision and Pattern Recognition, CVPR 1994*, pp. 593–600. IEEE (1994)
22. Yi, S., Labate, D., Easley, G.R., Krim, H.: A shearlet approach to edge analysis and detection. *IEEE Transactions on Image Processing* **18**(5), 929–941 (2009)